Electrically injected spin-polarized vertical-cavity surface-emitting lasers

M. Holub, J. Shin, S. Chakrabarti, and P. Bhattacharya[a)]
Department of Electrical Engineering and Computer Science, Solid State Electronics Laboratory, University of Michigan, Ann Arbor, Michigan 48109-2122

(Received 16 February 2005; accepted 8 July 2005; published online 24 August 2005)

We report the design, fabrication, and characterization of an electrically injected, spin-polarized, vertical-cavity surface-emitting laser. We have demonstrated spin injection from the ferromagnetic semiconductor (Ga,Mn)As into $In_{0.2}Ga_{0.8}As/GaAs$ quantum wells, spin transport across a distance of $\sim 0.25\ \mu m$ for temperatures ranging from 80 to 105 K, and spin detection through optical polarization measurements with coherent light emission. Controlled switching between right- and left-elliptically polarized modes is achieved with a maximum degree of circular polarization of 4.6% measured at 80 K. © *2005 American Institute of Physics*. [DOI: 10.1063/1.2035329]

Current communication systems rely on modulation of the amplitude and frequency of electromagnetic waves to transfer information, neglecting their polarization state. The ability to dynamically and continuously switch between orthogonal polarization states in semiconductor lasers offers an elegant method for secure communications over fiber optic cables as well as light-wave networks with enhanced bandwidth. Several methods for polarization control in vertical-cavity surface-emitting lasers (VCSELs) utilizing cavity[1,2] or mirror[3,4] anisotropy have recently been reported; however, these methods only succeed in stabilizing a desired polarization state over a particular range of operating conditions. Polarization modulation of coherent light emission still remains a formidable challenge, although a semiconductor device with such capability would be of great practical interest for cryptography, reconfigurable optical interconnects, and advanced optical switches and modulators. Here we report polarization modulation in an electrically injected, spintronic laser. Spin injection into InGaAs quantum wells (QWs) and subsequent coherent, elliptically polarized emission is achieved using a (Ga,Mn)As spin aligner embedded in a gain-guided VCSEL. Controlled polarization switching between left and right helicity is demonstrated using applied magnetic fields. We achieve spin-injection efficiencies of 4.6% at 80 K and device operation over the temperature range of 80–105 K.

The device structure, shown schematically in Fig. 1(a), was grown by molecular beam epitaxy on semi-insulating GaAs(001) substrates with an undoped 250 nm GaAs buffer layer. The spin-polarized VCSEL (spin-VCSEL) consists of a 29.5-pair, n-doped ($N_D = 5 \times 10^{18}\ cm^{-3}$) $Al_{0.8}Ga_{0.2}As/GaAs$ distributed Bragg reflector (DBR) stack for the bottom mirror; a full-wave cavity spacer of GaAs with an active region consisting of five, undoped, 5 nm $In_{0.2}Ga_{0.8}As$ QWs separated by 10 nm GaAs barriers; and a top mirror formed from one quarter-wave pair of p-doped ($N_A = 5 \times 10^{18}\ cm^{-3}$) $Al_{0.8}Ga_{0.2}As/Ga(Mn)As$ DBR and a 5-pair $ZnSe/MgF_2$ dielectric DBR stack. Our choice of an InGaAs/GaAs QW VCSEL design over a similar GaAs/AlGaAs QW VCSEL was motivated by two considerations. First, the smaller band gap of $In_{0.2}Ga_{0.8}As$ eliminates any spurious contribution to the optical polarization arising from reabsorption in the dichroic spin aligner of a top-emitting VCSEL. Second, our design provides a temperature-insensitive background polarization whose orientation is fixed along a ⟨110⟩ crystal axis.[5] This feature simplifies assessment of optical polarization changes due to spin injection from a magnetic contact.

For the present work, a thin (15 nm) low-temperature-annealed $Ga_{0.95}Mn_{0.05}As$ was placed in the top mirror and serves as the spin-aligner layer. It is well-known that (Ga,Mn)As—a p-type, ferromagnetic semiconductor[6,7] develops spontaneous magnetization at temperatures below its Curie temperature (T_C), which gives rise to a large Zeeman splitting of the valence bands to create spin-polarized holes. Details of the low-temperature (LT) epitaxy[8] and post-

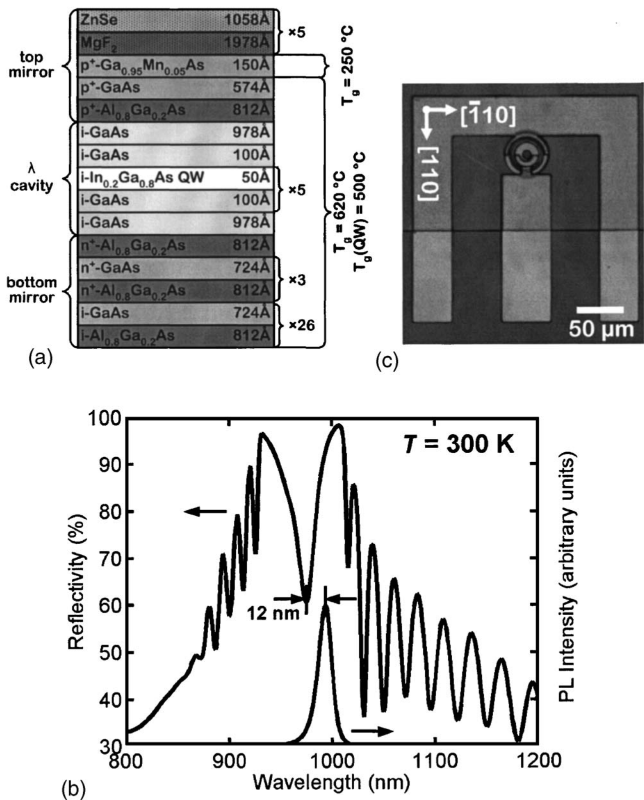

FIG. 1. (a) Device heterostructure showing the doping profile, growth temperatures, and layer thicknesses of the top and bottom mirrors, λ cavity, and active region; (b) room-temperature reflectivity and photoluminescence (PL) spectra of the spin-VCSEL heterostructure prior to fabrication. A +12 nm offset between the reflectivity dip and PL peak wavelengths at 300 K was introduced to optimize the spin-VCSEL performance at 100 K; (c) image of a fabricated spin-VCSEL with ground-signal-ground contacts.

[a)]Electronic mail: pkb@eecs.umich.edu

 © 2005 American Institute of Physics

growth annealing[9] processes required for ferromagnetic behavior in (Ga,Mn)As with large magnetization levels and T_C have been reported previously. It is important to note, however, that the nonequilibrium LT-growth mode favors formation of native and impurity-related defects, particularly arsenic antisites[10] (As_{Ga}) and manganese interstitials[11] (Mn_I), in high concentrations ($>10^{19}$ cm^{-3}). Recent investigations of the As_{Ga} defect in LT-Ga(Mn)As[12,13] and LT-AlGaAs[14] epilayers have revealed large sub-band-gap absorption coefficients and refractive index changes as compared to layers grown under normal conditions. These effects have important consequences for VCSEL design and operation insomuch as they complicate growth of LT layers having a desired optical thickness and increase the mirror loss. In this context, we have examined Ga(Mn)As/AlAs Bragg mirrors containing LT-grown layers. Dramatic distortion of the reflectivity spectra and a reduced peak reflectivity were observed in these mirrors, presumably owing to As_{Ga} defect-induced absorption. Simulations performed using a transform matrix formulation accurately reproduce these experimental findings when the values for refractive index and absorption coefficient change reported in Refs. 12 and 14 are assumed. Moreover, initial spin-VCSEL heterostructures were prepared with an n-doped $Al_{0.8}Ga_{0.2}As$/GaAs bottom mirror, λ cavity, and top mirror comprised of a single $Al_{0.8}Ga_{0.2}As$:Be (81.2 nm)/$Ga_{0.95}Mn_{0.05}As$ (75.6 nm) DBR. These heterostructures exhibited 8.7% degradation in peak reflectivity as compared to structures grown entirely at a high temperature, and lasing operation was not observed for the final processed devices. To circumvent this problem and maintain the optical quality of the top mirror, we use the thinnest possible (Ga,Mn)As spin aligner and place this layer at the top of the heterostructure to minimize the amount of LT-grown material.

Despite extensive research on magnetic semiconductors, the ferromagnetic transition temperature of spin aligners compatible with Al(Ga)As/GaAs heterostructure devices remains undesirably low ($\leqslant$160 K).[15] Thus, in order for spin injection to occur from (Ga,Mn)As, the spin-VCSEL must be carefully designed for low-temperature operation by accounting for the temperature dependence of the laser cavity resonance wavelength, λ_R, and material gain peak (or luminescence peak) wavelength, λ_P. Suitable selection of the gain offset wavelength, $\lambda_P-\lambda_R$, can minimize the threshold current and provide maximum output power over a desired temperature range. Thus, for spin-VCSEL operation at 100 K, we introduced a gain offset of +12 nm at 300 K [Fig. 1(b)] as evidenced by the wavelength separation between the QW photoluminescence (PL) peak and reflectivity dip for the epitaxial wafer. Finally, spin-VCSELs of varying mesa diameters were fabricated using standard optical lithography, wet etching, polyimide planarization and passivation, metallization, and dielectric electron-beam evaporation techniques. An image of a representative, fabricated spin-VCSEL is shown in Fig. 1(c). Nonmagnetic control devices with a heavily-Be-doped GaAs ($N_A=5\times10^{18}$ cm^{-3}) layer replacing the (Ga,Mn)As spin aligner were also epitaxially grown and fabricated to verify spin injection.

Radiative recombination of spin-up and spin-down holes yields two, coherently coupled lasing transitions producing left- and right-circularly polarized light, respectively. In a nonmagnetic VCSEL these two lasing modes are pumped equally from equal injection of spin-up and spin-down carriers. Consequently, two equal and in-phase circularly polarized modes are generated which admix to form linearly polarized emission. Polarization discrimination in spin-polarized light sources arises directly from well-known selection rules[16] for the conservation of angular momentum and preferential injection of either spin-up or spin-down carriers from a magnetic contact or a spin-aligning layer. The selection rules directly relate the spin orientation of active region carriers to the helicity of photons emitted upon their radiative recombination. A distance of ~250 nm separates the spin aligner from the active region in our spin-VCSEL. Hole spin injection for $T<52$ K and transport across distances greater than 200 nm has already been demonstrated in InGaAs/GaAs/GaMnAs spin-polarized light-emitting diodes (spin-LEDs)[17] despite rapid hole spin relaxation rates and transport through heterointerfaces. Hole spin relaxation times of 6.5 ps have been reported for intrinsic $In_{0.2}Ga_{0.8}As$/GaAs QWs at 1.7 K.[18] We note, however, that for an InGaAs/GaAs QW VCSEL operated above threshold the carrier lifetime is significantly reduced due to stimulated emission. So, spin dephasing is expected to play a minor role, and larger optical polarizations and higher operating temperatures should be attainable in a spin laser than for comparable spin-LEDs.[19]

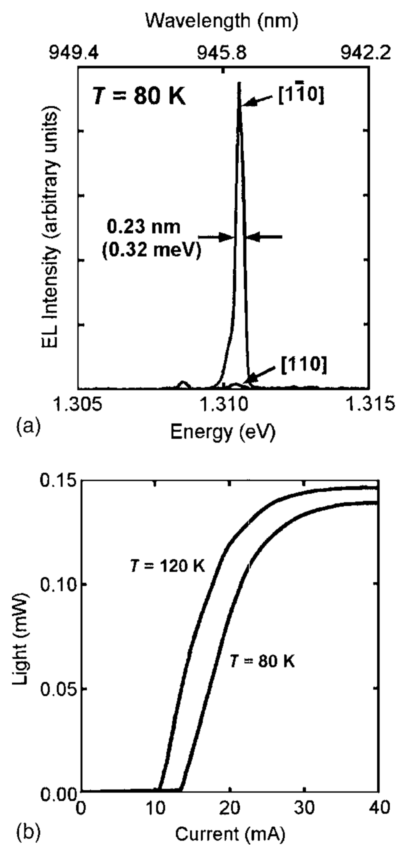

FIG. 2. (a) Linear-polarization-resolved electroluminescence spectra [full width at half-maximum, FWHM=0.23 nm (0.32 meV)] of the spin-VCSEL at 80 K; (b) light vs current plots of a typical VCSEL having an 8 μm aperture diameter (24 μm outer diameter) obtained at T=80 and 120 K.

The spin-VCSELs were mounted in a magneto-optical cryostat and characterized in the Faraday geometry with a variable magnetic field applied along the surface normal, which is the hard axis of (Ga,Mn)As. Before magnetizing the device in an applied magnetic field, the degree of linear polarization, Π_{LP}, of the VCSEL emission was assessed

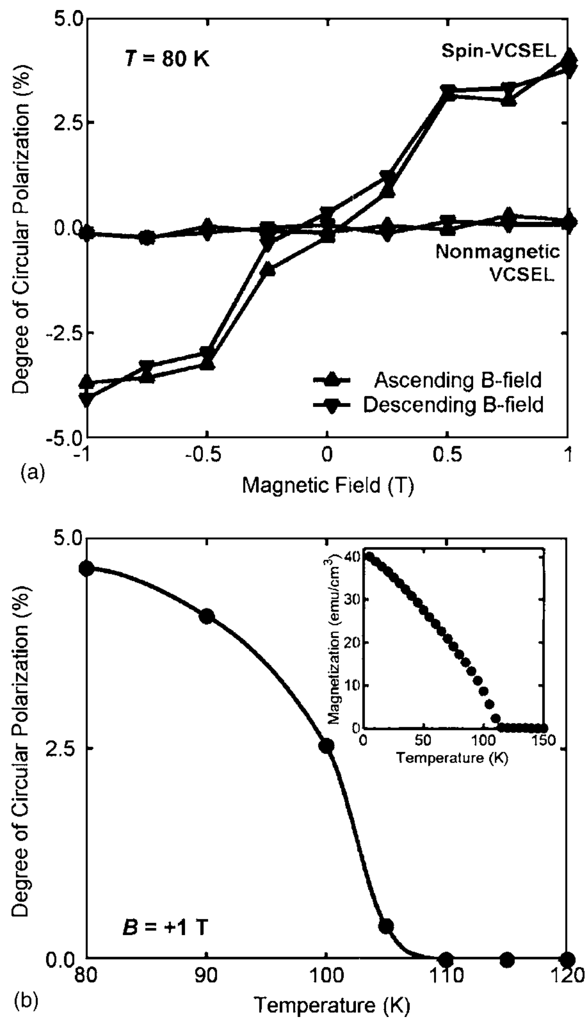

FIG. 3. (a) Field dependence of the degree of circular polarization demonstrating helicity modulation of the elliptically polarized emission at 80 K using applied magnetic fields; (b) temperature dependence of the degree of circular polarization demonstrating spin injection and device operation from 80–105 K. Inset shows the in-plane, field-cooled magnetization vs temperature for the low-temperature-annealed laser heterostructure.

through linear-polarization-resolved electroluminescence (EL) measurements. As shown in Fig. 2(a), maximum and null intensities were measured along the $[1\bar{1}0]$ and $[110]$ crystallographic directions for continuous-wave operation above threshold. This finding indicates highly linearly polarized emission with $\Pi_{LP}=(I^{[1\bar{1}0]}-I^{[110]})/(I^{[1\bar{1}0]}+I^{[110]})=0.97$ and confirms coherent (or lasing) optical output. A full width at half maximum (FWHM) of 0.23 nm (0.32 meV) for the EL spectrum was measured using a silicon charge coupled device attached to a spectrometer. Light versus current measurements [Fig. 2(b)] find a threshold current of 13.5 mA at 80 K for a spin-VCSEL having an 8 μm aperture diameter (24 μm outer diameter).

Detection of spin-polarized injection from the (Ga,Mn)As spin aligner into the QW active region was accomplished using a quarter-wave plate and linear polarizer to analyze the degree of circular polarization, Π_{CP}, for both the spin- and nonmagnetic- VCSELs. Figures 3(a) and 3(b) show $\Pi_{CP}=(I^{RCP}-I^{LCP})/(I^{RCP}+I^{LCP})$ as a function of applied magnetic field and temperature, respectively, where I^{RCP} and I^{LCP} are the energy-integrated intensities of right- and left- circularly polarized components for the dominant laser mode. The inset to Fig. 3(b) shows the temperature-dependent, in-plane, field-cooled magnetization of the low-temperature-annealed spin-VCSEL heterostructure measured in a 50 Oe field using a superconducting quantum interference device (SQUID) magnetometer. A maximum Π_{CP} of 4.6% was measured at 80 K in the presence of +1 T. A nonzero Π_{CP} was observed over the temperature range of 80–105 K, demonstrating spin injection and device operation up to a temperature slightly below the measured T_C of the spin aligner (T_C=113 K). The presence of hysteretic polarization with a field dependence similar to the out-of-plane magnetization of (Ga,Mn)As in the spin-VCSEL and absence in the control VCSEL is indicative of hole spin injection over a distance of ~250 nm at temperatures $T<110$ K.

Using ferromagnetic semiconductors to inject spin-polarized carriers, we have demonstrated controllable modulation of elliptically polarized, coherent light in a VCSEL with the helicity depending on the spin orientation of the active region hole population as determined by the magnetization of the spin aligner. Our experiment proves that the concept of spin injection applies equally well for semiconductor lasers as it does for LEDs.

This work is being supported by the Office of Naval Research under Grant No. N00014-02-1-0899 and the Army Research Office (MURI Program) under Grant No. DAAD19-99-1-0198. M.H. acknowledges support under a National Science Foundation Graduate Research Fellowship.

[1]T. Yoshikawa, H. Kosaka, K. Kurihara, M. Kajita, Y. Sugimoto, and K. Kasahara, Appl. Phys. Lett. **66**, 908 (1995).
[2]K. D. Choquette and R. E. Leibenguth, IEEE Photonics Technol. Lett. **6**, 40 (1994).
[3]T. Mukaihara, N. Ohnoki, Y. Hayashi, N. Hatori, F. Koyama, and K. Iga, IEEE J. Sel. Top. Quantum Electron. **1**, 667 (1995).
[4]M. Shimuzi, T. Mukaihara, F. Koyama, and K. Iga, Electron. Lett. **27**, 163 (1991).
[5]K. D. Choquette, R. P. Schneider, Jr., K. L. Lear, and R. E. Leibenguth, IEEE J. Sel. Top. Quantum Electron. **1**, 661 (1995).
[6]T. Dietl and H. Ohno, MRS Bull. **28**, 714 (2003).
[7]H. Ohno, J. Magn. Magn. Mater. **200**, 110 (1999).
[8]A. Shen, H. Ohno, F. Matsukura, Y. Sugawara, N. Akiba, T. Kuroiwa, A. Oiwa, A. Endo, S. Katsumoto, and Y. Iye, J. Cryst. Growth **175-176**, 1069 (1997).
[9]K. C. Ku, S. J. Potashnik, R. F. Wang, S. H. Chun, P. Schiffer, N. Samarth, M. J. Seong, A. Mascarenhas, E. Johnston-Halperin, R. C. Myers, A. C. Gossard, and D. D. Awschalom, Appl. Phys. Lett. **82**, 2302 (2003).
[10]X. Liu, A. Prasad, J. Nishio, E. R. Weber, Z. Liliental-Weber, and W. Walukiewicz, Appl. Phys. Lett. **67**, 279 (1995).
[11]K. M. Yu, W. Walukiewicz, T. Wojtowicz, I. Kuryliszyn, X. Liu, Y. Sasaki, and J. K. Furdyna, Phys. Rev. B **65**, 201303(R) (2002).
[12]S. U. Dankowski, P. Kiesel, B. Knüpfer, M. Kneissl, G. H. Döhler, U. D. Keil, D. R. Dykaar, and R. F. Kopf, Appl. Phys. Lett. **65**, 3269 (1994).
[13]A. Wolos, M. Kaminska, M. Palczewska, A. Twardowski, X. Liu, T. Wojtowicz, and J. K. Furdyna, J. Appl. Phys. **96**, 530 (2004).
[14]S. U. Dankowski, D. Streb, M. Ruff, P. Kiesel, M. Kneissl, B. Knüpfer, G. H. Döhler, U. D. Keil, C. B. Sørenson, and A. K. Verma, Appl. Phys. Lett. **68**, 37 (1996).
[15]D. Chiba, K. Takamura, F. Matsukura, and H. Ohno, Appl. Phys. Lett. **82**, 3020 (2003).
[16]*Optical Orientation*, edited by F. Meier and B. P. Zakharchenya (Elsevier Science, Amsterdam, 1984).
[17]Y. Ohno, D. K. Young, B. Beschoten, F. Matsukura, H. Ohno, and D. D. Awschalom, Nature (London) **402**, 790 (1999).
[18]T. Amand, B. Dareys, B. Baylac, X. Marie, J. Barrau, M. Brousseau, D. J. Dunstan, and R. Planel, Phys. Rev. B **50**, 11624 (1994).
[19]J. Rudolph, D. Hägele, H. M. Gibbs, G. Khitrova, and M. Oestreich, Appl. Phys. Lett. **82**, 4516 (2003).